# Compound Formation and Phase Equilibria in the System Li$_4$SiO$_4$–LiGaSiO$_4$

P. QUINTANA* AND A. R. WEST

*University of Aberdeen, Department of Chemistry, Meston Walk, Aberdeen AB9 2UE, United Kingdom*

Four new phases have been synthesized and characterized in the system Li$_4$SiO$_4$–LiGaSiO$_4$. Three have the ideal formula Li$_5$GaSi$_2$O$_8$, one of which, δ, is a stoichiometric phase and the other two, β and γ, form in addition a range of solid solutions to either side of this composition. The β phase appears to be structurally related to γ-Li$_3$PO$_4$ and the γ phase is a low-temperature ordered form of β. The β ⇌ γ transition is similar to that observed in Li$_4$Zn(PO$_4$)$_2$. The fourth new phase, α, is a solid-solution phase structurally related to γ-LiAlO$_2$. Li$_4$SiO$_4$ forms an extensive range of solid solutions which gradually transform to the α structure with increasing LiGaSiO$_4$ content. Low-temperature, ordered forms of the α solid solutions and the Li$_4$SiO$_4$ solid solutions have been partially characterized. The complete phase diagram Li$_4$SiO$_4$–LiGaSiO$_4$ has been determined; the system behaves as binary except at compositions close to LiGaSiO$_4$ at which LiGa$_5$O$_8$ appears in partially melted samples. © 1989 Academic Press, Inc.

## Introduction

Lithium aluminosilicates are widely used as the basis for glass-ceramics and ceramics with zero coefficient of thermal expansion (*1*). Only limited studies have been reported on the existence, structure, and properties of lithium gallosilicates, however. A study of compound formation on the join SiO$_2$–LiGaSiO$_4$ showed the formation of several phases and solid solutions, both thermodynamically stable and metastable, some of which are structurally similar to the lithium aluminosilicates (*2*). The conductivity of some of these phases has been reported (*3*): LiGaSiO$_4$ has a low level of electronic conductivity which contrasts with LiAlSiO$_4$ which is a one-dimensional Li$^+$ ion conduc-

tor at high temperatures. LiGaSi$_2$O$_6$ and its solid solutions exhibit a low level of Li$^+$ ion conductivity. Lithium orthosilicate, Li$_4$SiO$_4$, is the parent structure of lithium ion conducting solid electrolytes which have been proposed for solid-state battery applications (*4–6*). The present study reports the formation of several new phases and solid solutions on the join Li$_4$SiO$_4$–LiGaSiO$_4$.

## Experimental

Starting materials were Li$_2$CO$_3$, Ga$_2$O$_3$, and SiO$_2$. All were high-purity reagents and were used directly from the bottle: from weight loss checks, drying was found to be unnecessary. Mixtures were prepared in 5 to 10-g amounts, mixed thoroughly with an agate mortar and pestle, and fired in Au foil boats, initially at 600–800°C to drive off CO$_2$. Various firing schedules were used to

* Permanent address: Facultad de Quimica, UNAM, Mexico DF 04510, Mexico.

complete the reactions and these are described at appropriate stages under Results. X-ray powder diffraction patterns were recorded with a Philips Hägg Guinier camera, $CuK\alpha_1$ radiation, 1.54059 Å; for accurate $d$-spacing measurements, either KCl or $SiO_2$, quartz was added as an internal standard. Differential thermal analysis, DTA, used a Stanton–Redcroft 674, 1640°C instrument.

## Results

### Phases and Solid Solutions on the Join $Li_4SiO_4–LiGaSiO_4$: General Comments

Several phases and solid solutions form on this join, as shown by the rather complicated phase diagram in Fig. 1. Some are stable only at high temperatures, others

only at low temperatures. Some are stoichiometric phases; others form extensive solid solution series. Various phase transitions occur, the temperatures for which are very composition-dependent.

All of these phases are new and a major difficulty in the early stages of this project was to locate their compositions. This was for two reasons: samples were prone to lithia loss by volatilization on prolonged heating, of small samples especially, at temperatures above ~1000°C; in order to form some of the phases, long reaction times, 1–2 days, at high temperatures, 1000–1100°C, were found necessary in order to obtain complete reaction and single-phase products. In the initial stages, samples were reacted at 800–1000°C for a few hours and, while it was clear that new
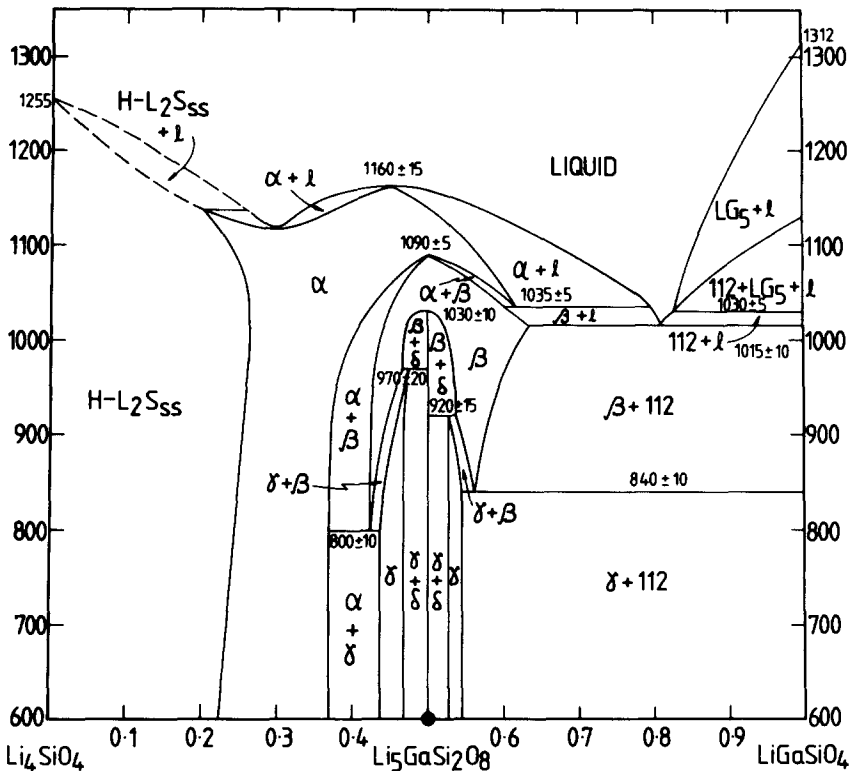


FIG. 1. Phase diagram $Li_4SiO_4–LiGaSiO_4$. $L_2Sss$, $Li_4SiO_4$ solid solutions; $LG_5$, $LiGa_5O_8$; 112, LiGa $SiO_4$; l, liquid.

phases were forming, a self-consistent pattern did not emerge. It was then suspected that at least some of the new phases may not lie on this particular join but may be elsewhere in the ternary system Li$_2$O–Ga$_2$O$_3$–SiO$_2$. During a systematic study of the ternary system and while trying to establish the subsolidus compatibility relations, it was realized that slowness of the reaction rates was a major factor in yielding discrepant results. It was also clear that many of the new materials have compositions that do, in fact, lie on the join Li$_4$SiO$_4$–LiGaSiO$_4$.

In order to establish the compositions and stabilities of the new phases and ultimately determine the phase diagram, it was clear that the conditions of heating required to obtain complete reaction depended very much on composition and the particular phase product. For compositions close to Li$_4$SiO$_4$ and containing up to about 40% LiGaSiO$_4$, reaction occurred in 1 day at ~900°C. For compositions around 40–60% LiGaSiO$_4$, several days at 1000°C were required in order to obtain the low-temperature δ phase. But, in order to obtain the high-temperature phases, several hours at temperatures of 1050–1150°C, sometimes followed by quenching of the sample, were required.

In general, samples were prepared from prereacted mixtures of Li$_4$SiO$_4$ and LiGaSiO$_4$. These were pelleted and the pellets were covered with loose powder of the same mixture and reacted in large Pt envelopes. The purpose of the covering powder was to prevent lithia loss from the pellets; only the pellets were used for X-ray analysis and subsequent experiments. The conditions of reaction used for each composition are given in Table I. Pellet fragments were used for further heat treatment experiments, to determine solid-solution extents, thermal stabilities, etc., and to construct the phase diagram shown in Fig. 1. These experiments are detailed in Table II. The

characteristic features of each of the new phases and solid solutions is discussed next.

### The α Phase

This is a solid-solution phase of general formula Li$_{4-3x}$Ga$_x$SiO$_4$. For compositions in the range ~0.25 < $x$ < ~0.35, it is stable at all temperatures below melting (Fig. 1) either as the α form or as low-temperature α′, α″ forms. At high temperatures, close to melting, it has a more extensive compositional extent, ~0.20 < $x$ < ~0.60. It is not clear from the phase diagram whether the α phase has an ideal composition or not. Thus, its maximum melting temperature appears to occur not at a simple composition but instead, at around $x = 0.45$. On the other hand, the compositions which are stable at lower temperatures have lower $x$ indicating that perhaps $x = 0.33$ is the ideal composition. In order to determine the ideal composition of α, if indeed there is one, crystallographic studies are required.

The X-ray powder pattern of the α phase is fairly simple, indicating a high-symmetry structure. It is very similar to that of γ-LiAlO$_2$, which is tetragonal and the powder pattern has been indexed using that of LiAlO$_2$ as a guide. For one composition, $x = 0.35$, the complete powder pattern was measured with an internal standard and accurate lattice parameters obtained by least-squares refinement (Table III). Significant changes in the powder pattern occur with changing composition, as shown by the variation in lattice parameters (Fig. 2): $a$ decreases but $c$ increases with $x$. The data show some scatter, but for these measurements, the X-ray films were used without an internal standard; the lattice parameters were obtained from the positions of the 020 and 012 lines.

From the similarity of the powder pattern of the α phase to that of γ-LiAlO$_2$, it seems that these could be isostructural. This

TABLE I

CONDITIONS OF SYNTHESIS: PELLETED SAMPLES BUFFERED (COVERED) WITH PREVIOUSLY SINTERED POWDER OF THE SAME COMPOSITION

| Composition $Li_{4-3x}Ga_xSiO_4$ | $T$ (°C) | $t$ (hr) | Phase(s) produced | Composition $Li_{4-3x}Ga_xSiO_4$ | $T$ (°C) | $t$ (hr) | Phase(s) produced |
|---|---|---|---|---|---|---|---|
| $x = 0.1$ | 900 | 18 | | | 1025 | 24 | |
| | 1000 | 18 | $L_2Sss$ | | 1050 | 24 | $\alpha + \beta$ |
| 0.15 | 900 | 19 | | 0.48 | 950 | 24 | |
| | 1000 | 24 | $L_2Sss$ | | 1000 | 72 | |
| 0.2 | 900 | 19 | | | 1020 | 24 | |
| | 950 | 36 | | | 1040 | 24 | $\beta/\gamma$ |
| | 1000 | 24 | $L_2Sss$ | 0.5 | 950 | 43 | |
| 0.22 | 925 | 24 | | | 1000 | 72 | |
| | 1000 | 5 | | | 1025 | 24 | |
| | 1030 | 23 | $L_2Sss$ | | 1050 | 24 | $\gamma$ |
| 0.25 | 900 | 19 | | 0.52 | 1000 | 72 | |
| | 950 | 36 | | | 1050 | 48 | $\gamma$ |
| | 1000 | 24 | $L_2Sss$ | 0.55 | 1000 | 48 | |
| | 950 | 43 | | | 1025 | 48 | |
| | 1000 | 72 | $L_2Sss$ | | 1040 | 36 | $\beta$ |
| 0.28 | 925 | 24 | | 0.57 | 800 | 24 | |
| | 1000 | 5 | | | 1000 | 174 | $\beta$ |
| | 1030 | 23 | $L_2Sss$ | 0.6 | 900 | 20 | |
| 0.3 | 900 | 48 | | | 1000 | 96 | $\beta$ |
| | 1000 | 22 | | 0.65 | 950 | 43 | |
| | 1050 | 20 | $\alpha$ | | 1000 | 72 | $\beta$ + trace 112 |
| 0.35 | 900 | 18 | | 0.7 | 900 | 20 | |
| | 1000 | 24 | $\alpha$ | | 1000 | 96 | 112 + $\beta$ |
| | 1000 | 144 | $\alpha$ | 0.75 | 950 | 43 | |
| 0.4 | 900 | 24 | | | 1000 | 72 | 112 + $\beta$ |
| | 1000 | 48 | | 0.8 | 900 | 69 | |
| | 1050 | 24 | $\alpha$ | | 1000 | 60 | 112 + $\beta$ |
| | 850 | 15 | | 0.85 | 900 | 24 | |
| | 950 | 24 | | | 1000 | 24 | |
| | 1000 | 8 | $\alpha$ | | 1015 | 24 | 112 + $\beta$ |
| 0.42 | 1000 | 144 | | 0.9 | 850 | 24 | |
| | 1030 | 20 | $\alpha$ | | 950 | 24 | |
| 0.45 | 950 | 43 | | | 1000 | 60 | 112 + $\beta$ |
| | 1000 | 72 | | | | | |

*Note.* $L_2Sss$, $Li_4SiO_4$ solid solution; 112, $LiGaSiO_4$.

would apply strictly only at the composition $x = 0.5$, where the cation:anion ratio is unity and would indicate an ideal composition of $x = 0.5$ for $\alpha$. The crystal structure of $\gamma$-$LiAlO_2$ (7) contains cations in tetrahedral sites in an oxide ion array which is intermediate between hexagonal close packed and tetragonal packed (8, 9). Re-

writing $\gamma$-$LiAlO_2$ as $\gamma$-$Li_4Al_4O_8$ and comparing this with the $x = 0.5$ composition, $Li_5GaSi_2O_8$, the replacement mechanism for the two phases to be isostructural is

$$4Al^{3+} \rightleftharpoons Li^+ + Ga^{3+} + 2Si^{4+}.$$
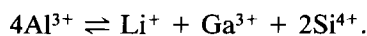
All cations are presumed located in tetrahedral sites for $x = 0.5$. For other composi-

## TABLE II

### RESULTS OF HEATING EXPERIMENTS IN THE SYSTEM Li$_4$SiO$_4$–LiGaSiO$_4$

| T (°C) | t (hr) | X-ray results | Comments | T (°C) | t (hr) | X-ray results | Comments |
|---|---|---|---|---|---|---|---|
| | | *x* = 0.1 | | 1027 | 1.75 | α | |
| 1150 | 0.66 | L₂Sss | *d*, Partial melting | 1015 | 3.5 | α | |
| 1150 | 0.5 | L₂Sss | *d* | 977 | 5 | α | |
| 1125 | 0.42 | L₂Sss | *d* | 852 | 22 | α | |
| 1100 | 0.66 | L₂Sss | *d* | 800 | 18 | α | *d* |
| 1000 | 12 | L₂Sss | *d* | 700 | 23 | α | *a,d* |
| | | *x* = 0.15 | | 601 | 16.5 | α | *a* |
| 1150 | 0.66 | L₂Sss | *d*, Sample melted | 500 | 24 | α | *a,c* |
| 1130 | 0.75 | L₂Sss | *d* | 300 | 18 | α″ | *a,c* |
| 1125 | 0.42 | L₂Sss | *d* | | | *x* = 0.3 | |
| 1080 | 1 | L₂Sss | *c* | 1159 | 0.33 | α | Sample melted |
| 700 | 20 | L₂Sss | *c* | 1140 | 1 | α | Sample melted |
| 600 | 16 | L₂Sss | *c,a* | 1128 | 0.5 | α | Partial melting |
| 450 | 32 | L₂S′ | *c,a* | 1097 | 0.5 | α | |
| 400 | 18 | L₂S′ | *c,a* | 1090 | 17 | α | |
| 400 | 12 | L₂S′ | *a,d* | 1077 | 0.5 | α | |
| | | *x* = 0.2 | | 1069 | 14 | α | |
| 1200 | 0.5 | α | *d* | 1048 | 0.5 | α | |
| 1150 | 1.16 | L₂Sss | *d*, Partial melting | 1031 | 0.5 | α | |
| 1100 | 0.66 | L₂Sss | *d* | 1009 | 0.5 | α | |
| 1080 | 1 | L₂Sss | *c* | 850 | 144 | α | *d* |
| 1030 | 17 | L₂Sss | *c* | 757 | 70.5 | α | *a* |
| 700 | 25 | L₂Sss | *c* | 700 | 24 | α | *c* |
| 500 | 25 | L₂Sss + L₂S′ | *c,a* | 650 | 23.5 | α | *c,a* |
| 450 | 20 | L₂S′ | *c,a* | 600 | 28.5 | α | *c,a* |
| 400 | 24 | L₂S′ | *c,a* | 500 | 23 | α′ | *c,a* |
| 400 | 12 | L₂S′ | *a,d* | 450 | 16.5 | α′ | *c,a* |
| | | *x* = 0.22 | | 400 | 24.5 | α′ | *c,a* |
| 1152 | 0.16 | | Melting | 300 | 23 | α″ | *c,a* |
| 1129 | 0.25 | L₂Sss | Partial melting | 900 | 2 | α | *c,a* |
| 1110 | 0.16 | L₂Sss | | | | *x* = 0.35 | |
| 1087 | 0.16 | L₂Sss | | 1160 | 0.66 | α | *d*, Sample melted |
| 1070 | 0.5 | L₂Sss | | 1140 | 1 | α | *d*, Partial melting |
| 1047 | 0.16 | L₂Sss | | 1115 | 4 | α | |
| 800 | 18 | L₂Sss | *d* | 1088 | 17 | α | |
| 601 | 16.5 | L₂Sss | *a* | 700 | 72 | α | *d* |
| 709 | 17.5 | L₂Sss | *a* | 601 | 16.5 | α′ | *c,a* |
| | | *x* = 0.25 | | 450 | 32 | α″ | *c,a* |
| 1160 | 0.66 | α | *d*, Sample melted | 400 | 68 | α″ | *c,a* |
| 1152 | 0.16 | α | Sample melted | 300 | 18 | α″ | *c,a* |
| 1129 | 0.25 | α | Partial melting | 900 | 66 | α | *c,a* |
| 1120 | 0.5 | α | *d* | | | *x* = 0.4 | |
| 1110 | 0.16 | α | | 1160 | 0.66 | α | *d*, Partial melting |
| 1087 | 0.16 | α | | 1140 | 1 | α | *d* |
| 1075 | 18.5 | L₂Sss | | 1096 | 0.5 | α | |
| 900 | 67.5 | α | *d* | 1078 | 0.5 | α | |
| 846 | 23 | α | | 1027 | 23.5 | α | |
| 757 | 70.5 | α | *a* | 803 | 89.5 | α + β | *a* |
| 990 | 1.5 | α | *a* | 900 | 67.5 | α + β | *d* |
| 800 | 21 | L₂Sss | *c* | 999 | 15.5 | α + β | *a* |
| 700 | 24 | L₂Sss | *c,a* | 803 | 89.5 | α + β | |
| 650 | 23.5 | L₂Sss | *c,a* | 757 | 70.5 | α + γ | *a* |
| 600 | 28.5 | L₄Sss | *c,a* | 700 | 24 | α + γ | *c* |
| 500 | 23 | L₂Sss + α | *c,a* | 757 | 70.5 | α + γ | |
| 450 | 16.5 | α | *c,a* | 700 | 24 | α + γ | *c* |
| 400 | 24.5 | α | *c,a* | 600 | 25 | α + γ | *c,a* |
| 300 | 23 | α″ | *c,a* | 500 | 22.5 | α + γ | *c,a* |
| | | *x* = 0.28 | | 700 | 72 | γ | *c* |
| 1152 | 0.16 | α | Sample melted | | | *x* = 0.42 | |
| 1129 | 0.25 | α | Partial melting | 1160 | 0.66 | α | *d*, Partial melting |
| 1110 | 0.16 | α | | 1088 | 17 | α | |
| 1087 | 0.16 | α | | 1115 | 4 | α | *a* |
| 1070 | 0.5 | α | | 1140 | 1 | α | *a* |
| 1047 | 0.16 | α | | 1027 | 23.5 | α | |

TABLE II—*Continued*

| T (°C) | t (hr) | X-ray results | Comments | T (°C) | t (hr) | X-ray results | Comments |
|---|---|---|---|---|---|---|---|
| 900 | 67.5 | α + β | d | 502 | 20.5 | γ + δ | a |
| 999 | 15.5 | α + β | a | 412 | 23 | γ + δ | a |
| 825 | 18 | α + β | | | | x = 0.52 | |
| 796 | 17 | α + γ | | 1021 | 17 | β | |
| 772 | 12.5 | α + γ | a | 1069 | 18 | β + γ | a |
| 700 | 72 | γ | c | 1088 | 17 | α | a,b |
| | | x = 0.45 | | 1100 | 17 | α | b |
| 1159 | 0.5 | α | Sample melted | 960 | 45 | β + δ | |
| 1095 | 0.5 | α | | 997 | 22 | β + δ | a |
| 1110 | 6 | α | a | 935 | 17 | β + δ | |
| 1130 | 3 | α | a | 905 | 14 | γ + δ | |
| 1160 | 3 | α | a, Sample melted | 855 | 17 | γ + δ | a |
| 1081 | 23 | α | | 876 | 20.5 | γ + δ | |
| 1058 | 20 | α | a | 800 | 70 | γ + δ | d,a |
| 1055 | 23.5 | α + β | | 650 | 66.5 | γ | d |
| 1089 | 6 | α | a | 602 | 6 | γ | |
| 1040 | 18 | α + β | | | | x = 0.55 | |
| 1050 | 4.58 | α + β | | 1200 | 0.25 | G | |
| 1024 | 23 | α + β | a | 1159 | 0.33 | α + G | |
| 1040 | 18 | α + β | a | 1095 | 0.5 | α | |
| 1026 | 63.5 | β | a | 1024 | 0.5 | β | |
| 1050 | 18 | α + β | | 1100 | 1.5 | α | a |
| 999 | 40.5 | β | a | 1110 | 2.5 | α + G | a |
| 898 | 17 | β + γ | a | 1130 | 2.67 | α + G | a |
| 850 | 14.25 | γ | a | 903 | 3 | β | |
| 1000 | 96 | β | c | 1063 | 16.5 | β + G | a |
| 1020 | 19 | β | a | 1180 | 1.5 | G | a |
| 650 | 66.5 | γ | d | 1069 | 14 | α + β | |
| | | x = 0.48 | | 1077 | 18.5 | α | a |
| 1081 | 17 | β + α | | 1047 | 0.5 | β | |
| 1100 | 9 | α | a,b | 1010 | 0.5 | β | |
| 1128 | 2.75 | α | a,b | 805 | 2 | β + γ | |
| 1144 | 2 | α | a,b, Partial melting | 822 | 1 | β + γ | a |
| 1169 | 1.5 | α + G | a,b, Sample melted | 786 | 2 | β + γ | a |
| 1092 | 19 | α | b | 751 | 2 | γ | a |
| 1069 | 18 | β | | 652 | 2.5 | γ + β | a,e |
| 1035 | 8 | β | a | 846 | 2 | β | a |
| 1021 | 17 | β + δ | | 776 | 23 | γ | |
| 960 | 45 | γ + δ | | 602 | 6 | γ + β | e |
| 997 | 22 | β + δ | a | 725 | 20 | γ | |
| 905 | 14 | γ + δ | | 1047 | 0.5 | β | |
| 855 | 17 | γ + δ | a | 800 | 22 | β | c,a |
| 800 | 70 | γ + δ | d,a | 700 | 21.5 | γ | c,e |
| 650 | 66.5 | γ + δ | d | 600 | 23.5 | γ + β | c,a,e |
| | | x = 0.5 | | 400 | 66 | γ + β | c,a,e |
| 1159 | 0.3 | α + G | b, Sample melted | 750 | 20 | γ + 112 | c,a |
| 1128 | 0.5 | α | b | | | x = 0.57 | |
| 1057 | 19 | β/γ | | 1200 | 0.25 | G | |
| 1065 | 18 | β/γ | a | 1178 | 0.25 | G | |
| 1075 | 3.25 | β/γ | a | 1115 | 4 | α + G | |
| 1085 | 4 | β/γ | a | 1094 | 0.58 | α + G | |
| 1094 | 4 | α | a,b | 1047 | 17 | β | |
| 1081 | 17 | β/γ | | 1069 | 18 | α | a |
| 1100 | 9 | α | a,b | 1088 | 17 | α + G | a |
| 1128 | 2.75 | α | a,b | 903 | 3 | β | |
| 1144 | 2 | α | a,b | 1063 | 16.5 | α | a |
| 1169 | 1.5 | α + G | a,b, Sample melted | 1034 | 16.75 | β | a |
| 1057 | 19 | β/γ | | 1049 | 3.5 | β | |
| 1034 | 16.5 | β | a | 1055 | 3.75 | α + β | a |
| 1020 | 3.5 | β + δ | a | 1063 | 16.5 | α | |
| 1008 | 17.5 | β + δ | a | 1028 | 4 | β | a |
| 905 | 17.5 | δ | a | 1047 | 17 | β | |
| 818 | 22.5 | δ | a | 800 | 22 | β | c,a |
| 700 | 42 | δ | c,a | 700 | 21.5 | β + γ | c,e |
| 668 | 23 | γ + δ | | 600 | 23.5 | β + γ | c,a,e |
| 603 | 19 | γ + δ | a | 400 | 66 | β + γ + 112 | c,a,e |

TABLE II—*Continued*

| T (°C) | t (hr) | X-ray results | Comments | T (°C) | t (hr) | X-ray results | Comments |
|---|---|---|---|---|---|---|---|
| 750 | 20 | γ + 112 | c | 1062 | 0.5 | α + G | |
| 725 | 20 | γ + β | e | 1040 | 7 | α + G | |
| 776 | 23 | γ | e | 1035 | 1 | α + β + G | e |
| 602 | 6 | γ + β + 112 | a,e | 1035 | 3.83 | α + trace G | a |
| 668 | 23 | γ + β | e | 1031 | 4 | β + trace G | |
| 603 | 19 | γ + β | a,e | 1047 | 0.5 | α + G | |
| 502 | 20.5 | γ + β | a,e | 1028 | 1 | β + trace G | a |
| 412 | 23 | γ + β | a,e | 1019 | 3.16 | β + trace G | a |
| | | *x = 0.6* | | 1010 | 3.75 | β + trace 112 | a |
| 1163 | 0.13 | α + G | e | 1024 | 2.66 | trace α + β + trace G | e |
| 1143 | 0.42 | α + G | e | 1023 | 5.16 | β + trace G | a |
| 1094 | 0.58 | α + G | | 1028 | 1 | β + trace G | |
| 1020 | 23 | β | d | 1000 | 28 | β + 112 | a |
| 1080 | 18 | α + trace G | d,a | 600 | 23.5 | γ + 112 | c |
| 1055 | 5.5 | α + trace G | | 400 | 66 | γ + 112 | c,a |
| 1046 | 22 | α + trace β | | 725 | 20 | γ + 112 | a |
| 1034 | 16.75 | β + trace G | a | 776 | 23 | γ + 112 | a |
| 1028 | 4.5 | β | | 800 | 6.5 | γ + 112 | a |
| 1044 | 3 | β | a | 851 | 28.5 | β + 112 | a |
| 1049 | 3.5 | α + β | a | 828 | 22 | γ + 112 | a |
| 1055 | 3.75 | α | a | | | *x = 0.75* | |
| 903 | 3 | β + trace 112 | | 1149 | 1.08 | G | |
| 1005 | 3 | β | a | 1082 | 2 | G + trace α | |
| 980 | 21.5 | β | a | 1058 | 1 | α + G | |
| 950 | 24 | β + trace 112 | a | 1050 | 6.5 | α + G | |
| 800 | 22 | β + 112 | c | 1040 | 7 | α + β + G | e |
| 700 | 21.5 | γ + 112 | c | 1040 | 18 | α + G | |
| 600 | 23.5 | γ + 112 + β | c,a,e | 1028 | 23 | 112 + β + G | e |
| 400 | 66 | γ + 112 | c,a | 1019 | 19.75 | 112 + β | |
| 1020 | 23 | β | d | 1013 | 23.75 | 112 + β | |
| 725 | 23 | β | a,e | | | *x = 0.8* | |
| 668 | 23 | γ + β | e | 1072 | 0.5 | G | |
| 603 | 19 | γ + β | a,e | 900 | 25 | β + 112 | a |
| 502 | 20.5 | γ + β | a,e | 1052 | 17 | G | |
| 412 | 23 | γ + β | a,e | 900 | 25 | β + 112 | a |
| | | *x = 0.65* | | 1028 | 23 | β + 112 + G | e |
| 1149 | 1.08 | G | | 1011 | 52 | β + 112 | |
| 1130 | 1.16 | G + trace α | | 1020 | 4 | β + 112 + trace G | e,a |
| 1098 | 2.33 | α + G | | | | *x = 0.85* | |
| 1027 | 17 | β + G | | 1082 | 1.5 | trace LG₅ + G | |
| 1044 | 18 | α + G | a | 1058 | 7 | trace LG₅ + G | |
| 1039 | 2.25 | α + G | | 1044 | 22 | 112 + LG₅ + G | |
| 1029 | 4.33 | β + trace G | | 1027 | 23.5 | 112 + β | |
| 1020 | 23 | β + trace G | | 999 | 15.5 | 112 + β | |
| 1010 | 15.67 | β + trace G | | | | *x = 0.9* | |
| 1002 | 23.75 | β + trace 112 | | 1155 | 1 | G | |
| 986 | 15 | β + trace 112 | | 1128 | 2 | trace LG₅ + G | |
| 965 | 22.5 | β + trace 112 | | 1097 | 2 | trace LG₅ + G | |
| 1020 | 23 | β + trace G | | 1080 | 4 | LG₅ + G | |
| 725 | 23 | β | a,e | 1052 | 17 | LG₅ + 112 + G | |
| 668 | 23 | β | e | 1040 | 7 | LG₅ + 112 + G | |
| 603 | 19 | β | a,e | 1028 | 23 | 112 + β + trace G | |
| 502 | 20.5 | trace γ + β | a,e | 1011 | 52 | 112 + β | |
| 412 | 23 | trace γ + β | a,e | 1020 | 4 | 112 + β | a |
| | | *x = 0.7* | | 1058 | 3.5 | LG₅ + 112 + G | a |
| 1119 | 1.25 | G | | | | | |
| 1080 | 0.5 | α + G | | | | | |

*Note.* Compositions are given as $x$ in the formula $Li_{4-3x}Ga_xSiO_4$. Unless stated otherwise, samples wrapped in Pt foil were heated in vertical tube furnaces, temperatures accurate to within 5°C, and quenched into Hg at the end of the experiment.

Abbreviations: $LG_5$, $LiGa_5O_8$; 112, $LiGaSiO_4$; α, α′, α″, $\alpha\text{-}Li_{4-3x}Ga_xSiO_4$; β, $\beta\text{-}Li_{5-x}Ga_{1+x}Si_2O_8$; γ, $\gamma\text{-}Li_{5-3x}Ga_{1+x}Si_2O_8$; δ, $\delta\text{-}Li_5GaSi_2O_8$; G, glass; $L_2Sss$, solid solution of $Li_4SiO_4$; $L_2S'$, low-temperature form of $Li_4SiO_4$ss.

[a] The sample used in this experiment had been used previously for the preceding experiment in the table.

[b] The X-ray powder pattern indicated a mixture of two α phases, of different composition.

[c] Temperature accurate to ±30°C; sample cooled in air at the end of the experiment.

[d] Furnace temperature accurate to ±20°C; sample quenched at the end of the experiment.

[e] The sample had not reached equilibrium in this experiment.

## TABLE III
### X-Ray Diffraction Data

| d(obs) | d(calc) | hkl | I | d(obs) | d(calc) | hkl | I |
|---|---|---|---|---|---|---|---|
| | $\alpha$-Li$_{4-3x}$Ga$_x$SiO$_4$[a]: $x = 0.35$ | | | 1.8272 | 1.8241 | 222 | 25 |
| | tetragonal, $a = 5.196 \pm 0.003$ Å | | | 1.8148[b] | 1.8148 | 312 | 10 |
| | $c = 6.186 \pm 0.010$ Å | | | 1.7994 | 1.8003 | 303 | 10 |
| 5.1950 | 5.1955 | 010 | <5 | | 1.7965 | 024 | |
| 3.9664 | 3.9786 | 011 | 80 | 1.6912 | 1.6918 | 313 | 10 |
| 3.6659 | 3.6738 | 110 | 15 | 1.6790 | 1.6793 | 106 | 10 |
| 3.1316 | 3.1588 | 111 | 30 | 1.6374 | 1.6382 | 304 | <5 |
| 2.6486 | 2.6578 | 012 | 75 | 1.6026 | 1.6022 | 320 | <5 |
| 2.5902 | 2.5978 | 020 | 100 | 1.5825 | 1.5837 | 321 | <5 |
| 2.1801 | 2.1751 | 211 | 5 | 1.5728[b] | 1.5728 | 032 | 10 |
| 1.8587 | 1.8578 | 122 | 10 | 1.5228 | 1.5250 | 206 | 45 |
| 1.8465 | 1.8369 | 220 | 10 | 1.4958 | 1.4932 | 007 | 15 |
| 1.7884 | 1.7982 | 113 | 5 | 1.4526 | 1.4556 | 323 | |
| 1.6724 | 1.6677 | 031 | <5 | | 1.4531 | 107 | |
| 1.5786 | 1.5794 | 222 | <5 | | 1.4507 | 133 | 25 |
| 1.5416 | 1.5423 | 123 | 5 | 1.4258 | 1.4296 | 017 | |
| 1.5067 | 1.5111 | 032 | 30 | | 1.4246 | 225 | |
| 1.4535 | 1.4510 | 132 | <5 | | 1.4244 | 026 | <5 |
| 1.3256 | 1.3262 | 033 | 5 | 1.3509 | 1.3502 | 404 | |
| 1.3094 | 1.3062 | 322 | <5 | | 1.3496 | 207 | 15 |
| 1.2963 | 1.2989 | 040 | 5 | 1.3303 | 1.3298 | 420 | 15 |
| 1.2878 | 1.2875 | 214 | 5 | | | | |
| | 1.2850 | 133 | | | $\gamma$-Li$_5$GaSi$_2$O$_8$[c] | | |
| 1.2287 | 1.2246 | 330 | <5 | | orthorhombic, $a = 12.526 \pm 0.006$ Å | | |
| 1.2001 | 1.2013 | 331 | <5 | | $b = 9.927 \pm 0.008$ Å | | |
| | 1.1976 | 042 | | | $c = 10.486 \pm 0.004$ Å | | |
| | | | | 7.783 | 7.780 | 110 | 25 |
| | | | | 6.251 | 6.263 | 200 | 55 |
| | $\beta$-Li$_{5-3y}$Ga$_{1+y}$Si$_2$O$_8$: $y = 0.14$ | | | | 6.248 | 111 | |
| | orthorhombic, $a = 6.308 \pm 0.004$ Å | | | 5.368 | 5.377 | 201 | 25 |
| | $b = 4.948 \pm 0.005$ Å | | | 4.347 | 4.348 | 112 | 30 |
| | $c = 10.453 \pm 0.004$ Å | | | 4.018 | 4.020 | 202 | 70 |
| 4.014 | 4.025 | 102 | 60 | 3.884 | 3.890 | 220 | 75 |
| 3.899 | 3.893 | 110 | 40 | 3.832 | 3.849 | 310 | 10 |
| 3.651 | 3.648 | 111 | 20 | 3.635 | 3.647 | 221 | 70 |
| 3.129 | 3.122 | 112 | 20 | 3.6099 | 3.6130 | 311 | 10 |
| 2.8489 | 2.8488 | 013 | 25 | | 3.6044 | 022 | |
| 2.6990 | 2.7005 | 202 | 80 | 3.1913 | 3.1991 | 130 | 25 |
| 2.6092 | 2.6132 | 004 | 50 | | 3.1884 | 113 | |
| 2.5971 | 2.5963 | 113 | 45 | 3.1119[d] | 3.1240 | 222 | 30 |
| 2.5802 | 2.5775 | 211 | 40 | | 3.1025 | 312 | |
| 2.4643 | 2.4739 | 020 | 100 | 3.0590 | 3.0599 | 131 | 30 |
| 2.4141 | 2.4142 | 104 | <5 | 2.8598 | 2.8578 | 023 | 10 |
| 2.3715 | 2.3704 | 212 | <5 | 2.6858[b] | 2.6884 | 402 | 100 |
| 2.1136 | 2.1141 | 213 | 25 | 2.6262 | 2.6215 | 004 | 80 |
| 1.9238 | 1.9257 | 015 | <5 | 2.5993[d] | 2.5999 | 223 | 30 |
| | 1.9213 | 123 | | | 2.5933 | 330 | |
| 1.9048 | 1.9029 | 311 | <5 | | 2.5875 | 313 | |

TABLE III—*Continued*

| d(obs) | d(calc) | hkl | I | d(obs) | d(calc) | hkl | I |
|---|---|---|---|---|---|---|---|
| 2.5652 | 2.5678 | 421 | 25 | | $\delta$-Li$_5$GaSi$_2$O$_8$[c] | | |
| 2.4816 | 2.4843 / 2.4816 | 114 / 040 | 100 | 7.3438 | | | 5 |
| | | | | 6.1946 | | | 10 |
| 2.3641 | 2.3639 | 422 | 20 | 5.9331 | | | 10 |
| 2.3292 | 2.3324 / 2.3245 | 403 / 332 | 5 | 4.6973 | | | 20 |
| | | | | 4.4952 | | | 85 |
| 2.2012 | 2.2040 | 512 | 5 | 3.8462 | | | 10 |
| 2.1744 | 2.1739 | 224 | 5 | 3.6508 | | | 40 |
| 2.1090 | 2.1109 | 423 | 20 | 3.4184 | | | 10 |
| 2.0806 | 2.0827 | 333 | 5 | 3.3807 | | | 20 |
| 2.0306 | 2.0277 | 134 | 10 | 3.3298 | | | 30 |
| 1.9909 | 1.9947 / 1.9887 | 513 / 205 | 5 | 3.3032 | | | 25 |
| | | | | 3.2394 | | | 5 |
| 1.9306[d] | 1.9319 / 1.9274 | 025 / 151 | 10 | 3.1769 | | | 15 |
| | | | | 3.0170 | | | 5 |
| 1.8941 | 1.8927 | 621 | 10 | 2.7045 | | | 100 |
| 1.8519[d] | 1.8631 / 1.8460 | 424 / 225 | 10 | 2.6604 | | | 10 |
| | | | | 2.4814 | | | 5 |
| 1.8275[d] | 1.8366 / 1.8235 | 152 / 442 | 15 | 2.3938 | | | 60 |
| | | | | 2.3672 | | | 25 |
| 1.8042 | 1.8065 / 1.8022 | 622 / 044 | 20 | 2.3471[d] | | | 30 |
| | | | | 2.3285 | | | 35 |
| 1.7350 | | | 10 | 2.1695[d] | | | 5 |
| 1.6870 | | | 5 | 2.0602 | | | 5 |
| 1.6336 | | | <5 | 1.8029 | | | 10 |
| 1.6023[d] | | | 10 | 1.7911 | | | 10 |
| 1.5636 | | | 25 | 1.7818 | | | 10 |
| 1.5278 | | | 40 | 1.7289[d] | | | 5 |
| 1.4962 | | | 25 | 1.6625 | | | 5 |
| 1.4523 | | | 15 | 1.6377 | | | <5 |
| 1.4449 | | | 10 | 1.5602 | | | 40 |
| 1.4323 | | | 10 | 1.3822 | | | 5 |
| 1.3518 | | | 5 | 1.3740 | | | 10 |
| 1.3443 | | | 10 | 1.3672 | | | 10 |
| 1.3259 | | | 5 | 1.3513 | | | 5 |
| 1.3178 | | | 20 | 1.3103 | | | 10 |
| | | | | 1.3010 | | | 15 |

[a] Quartz was used as internal standard.

[b] These peaks overlapped with the KCl internal standard; for them, the calculated d-spacing is given.

[c] KCl was used as internal standard.

[d] Closely spaced doublets.

tions, the likely replacement mechanism is $3\text{Li} \rightleftharpoons \text{Ga}$, giving rise to either Li interstitials or vacancies, depending on $x$.

For compositions in the range ~0.4 < $x$ < ~0.6, the $\alpha$ phase is stable only at high temperatures and transforms to other phases on cooling. These transformations are fairly slow, however, and can be avoided by cooling the samples quickly. For compositions around $x = 0.5$, the powder patterns of the quenched samples were poor with broad lines and some line split-
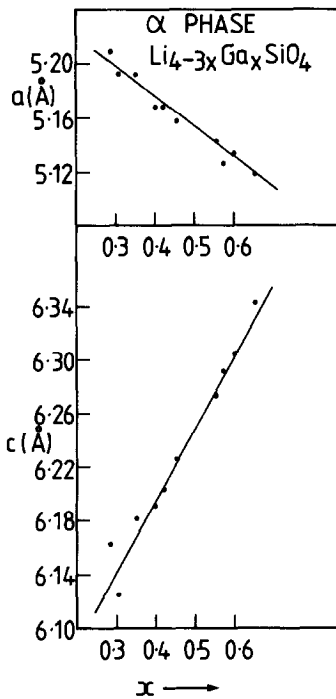
FIG. 2. Lattice parameters of tetragonal $\alpha$ phase as a function of composition.

nism and cannot be avoided, even by quenching the samples into mercury.

On annealing the $\alpha$ phase at low temperatures, 300–500°C, for compositions in the range 0.25–0.40, weak extra lines appear, indicating the probable formation of a superstructure. They appeared in two stages, giving the patterns labeled as $\alpha'$ and $\alpha''$. $\alpha'$ formed at 400–500°C and $\alpha''$ at 300–400°C, both with annealing times of 1–3 days. The patterns have not been measured accurately and indexed, but are shown as schematic line diagrams in Fig. 3.

### The $\beta$ Phase

This phase has the ideal stoichiometry, $Li_5GaSi_2O_8$. In addition, it forms a solid solution to either side of this composition with general formula, $Li_{5-3y}Ga_{1+y}Si_2O_8$. The compositional limits of the solid solution depend on temperature but are a maximum at $y = 0.27$ and 1015°C and at $y = -0.14$ and ~800°C. Note that the values of $y$ in this formula change at double the rate of the values of the composition scale in Fig. 1. Hence $y = 0.27$ corresponds to the composition 0.635 of Fig. 1 and $y = -0.14$ corresponds to composition 0.43.

The phase diagram, Fig. 1, shows that the $\beta$ phase is thermodynamically stable only for a limited range of high temperatures which is also very composition depen-

tings in the $\alpha$ pattern. It is believed that on cooling these samples, they enter a metastable immiscibility dome such that the high-temperature, homogeneous $\alpha$ phase separates into two phases, one of higher $x$ and one of lower $x$. This process may take place by a spinodal decomposition mecha-
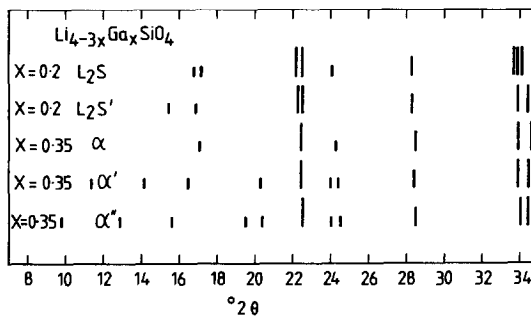


FIG. 3. Schematic X-ray line diagram.
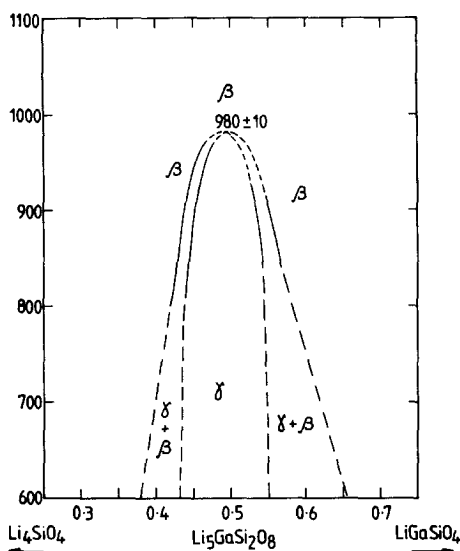
FIG. 4. Transformation between $\beta$ and $\gamma$ phases.

dent. Thus at $y = 0$, composition 0.50, $\beta$ is stable between 1030 and 1090°C, whereas to either side of this composition, its stability range moves to lower temperatures.

The effect of changing the temperature of the $\beta$ phase is to cause it to transform to other phases. At higher temperatures, the entire range of $\beta$ compositions transforms to the $\alpha$ structure. At lower temperatures, two kinds of behavior are observed. On fairly rapid cooling, transformation to the $\gamma$ phase occurs, as shown in Fig. 4. On prolonged annealing of samples of composition $y = 0.0$, at ~1000°C, transformation to the $\delta$ phase occurs and it is this behavior which is shown on the equilibrium phase diagram (Fig. 1). For compositions to either side of $y = 0.0$, transformation to the $\gamma$ phase represents the equilibrium situation and also appears on the phase diagram.

The characterization of the $\beta$ phase was possible using a combination of quenching experiments, X-ray diffraction, and DTA. For compositions to either side of, but not including, $y = 0.0$, $\beta$ could be quenched to room temperature. It was therefore possi-

ble to determine the stability field for $\beta$ at these compositions using quenching/X-ray diffraction. For compositions close to and including $y = 0.0$, $\beta$ converted to $\gamma$ during quenching. The extra X-ray reflections characteristic of $\gamma$ were broad in these quenched samples, however, which was a strong indication that the structure was indeed $\beta$ at the furnace temperature. Since the $\beta \rightleftharpoons \gamma$ transition was rapid, it could be followed by DTA, giving a clear endotherm on heating and an exotherm on cooling. The DTA results were consistent with the X-ray results: for that part of the composition range in which the transition could be followed by both X-ray diffraction and DTA, the transition temperatures obtained by the two techniques were in good agreement.

The X-ray powder pattern of $\beta$ shows strong similarities to those of $\gamma$-Li$_3$PO$_4$ (high form) (10) and Li$_4$Zn(PO$_4$)$_2$ (11). A similar-sized orthorhombic unit cell was used to index the data (Table III) and is consistent with unit cell contents of 2 formula units; again, an internal standard was added to measure accurately and index the complete pattern for one composition. The data are given for an off-stoichiometric composition, since this could be prepared readily as pure $\beta$ without transformation to $\gamma$. It seems likely that the structure is closely related to that of $\gamma$-Li$_3$PO$_4$ but crystallographic work is needed to confirm this since, although the cation:anion ratio is unity in both, three different cation types are present in $\beta$. One possibility is that the Si in $\beta$ occupies the P sites and that the Li, Ga in $\beta$ occupy the Li sites of Li$_3$PO$_4$, either in ordered or disordered fashion.

The powder pattern of the $\beta$ phase changed with composition. The lattice parameters were determined for a range of compositions, using a similar method to that indicated above for the $\alpha$ phase. These are shown in Fig. 5 for those compositions with $y > 0.0$; $a$ increases with increasing $y$, $b$ is unchanged, and $c$ decreases.
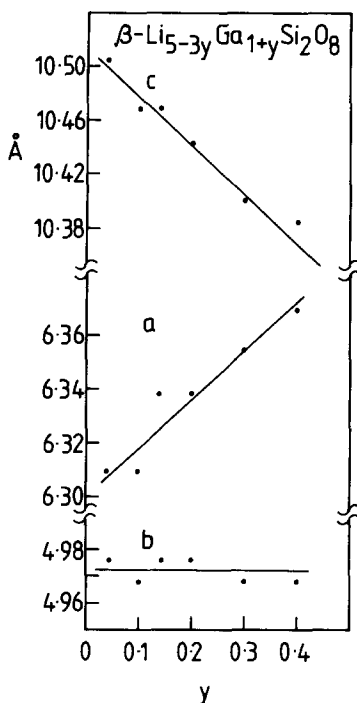
FIG. 5. Lattice parameters of orthorhombic $\beta$ phase as a function of composition.

## The $\gamma$ Phase

This phase also has the ideal stoichiometry $Li_5GaSi_2O_8$ and forms a limited range of solid solutions to either side. From the phase diagram studies, it is thermodynamically stable only at compositions to either side of, but not including, the ideal composition (Fig. 1). It is a low-temperature phase, forming below $\sim 980°C$ at the ideal composition and at lower temperatures for other compositions (Fig. 4).

It forms from the $\beta$ phase on cooling and the $\beta \rightleftharpoons \gamma$ transition appears to be an order–disorder transition, as shown by the appearance of extra lines in its powder pattern by comparison with that of the $\beta$ phase. The $\gamma$ phase powder pattern may be indexed on an orthorhombic unit cell similar to that of the $\beta$ phase but with $a$ and $b$ doubled (Table III). The structure of the $\gamma$

phase is not known but it appears to be based on that of $\gamma$-$Li_3PO_4$, with cation ordering. A similar ordering transition was observed in $Li_4Zn(PO_4)_2$ (11).

## The $\delta$ Phase

This phase also has the stoichiometry $Li_5GaSi_2O_8$ and appears to be a line phase with no significant solid solution. It is thermodynamically stable below $1030°C$ and appears on the phase diagram (Fig. 1). It does not form rapidly; several days heating at $1000°C$ are required to give a pure phase. Its structure is completely unknown; unindexed powder data are given in Table I.

## $Li_4SiO_4$ Solid Solutions

These have the formula $Li_{4-3x}Ga_xSiO_4$ and form over the range $0 < x < \sim 0.26$. Their compositional extent depends on temperature in a rather unusual manner. It is a maximum for $x \approx 0.26$ at $\sim 1000°C$ but at both higher and lower temperatures, the high $x$ compositions, $0.22–0.26$, transform reversibly to the $\alpha$ phase.

$Li_4SiO_4$ is a complex material with high-temperature polymorphism and several DTA peaks at temperatures of $\sim 400$ and $600–750°C$ (12). A comprehensive study of the polymorphism of the present $Li_4SiO_4$ solid solutions has not been made. For low $x$ compositions, DTA effects were also observed around $600–700°C$, attributed to a low–high transition in $Li_4SiO_4$, but these faded out with increasing $x$. With higher $x$ compositions, however, extra X-ray lines were observed on annealing solid solutions at $300–400°C$ for several hours or days and are probably due to the formation of a superstructure; this may or may not be related to the superstructure found in some $Li_4SiO_4$ crystals (13).

Considerable changes in the X-ray powder patterns of the $Li_4SiO_4$ solid solutions occur both with increasing $x$ and with an-

nealing. The patterns simplify somewhat in that split lines in $Li_4SiO_4$ gradually move closer together and some weak lines appear to disappear; however, other lines appear, especially in the low-temperature annealed samples. Some of these effects are illustrated as line diagrams in Fig. 3. Because of these complexities and the occurrence of several effects simultaneously, no attempt has been made to determine a complete diagram showing the polymorphism of these solid solutions or to index the powder data. It seems likely that the high-temperature solid solutions shown on the phase diagram have the high-$Li_4SiO_4$ structure and these have been labeled as such. The low-temperature ordered phase characterized by the appearance of extra X-ray lines has been labeled $L_2S'$ (Fig. 3).

The transition from the $Li_4SiO_4$ structure to the $\alpha$ phase structure with increasing $x$ appears to be continuous. There was no evidence from the phase diagram studies of a two-phase region separating the two solid solution fields. In addition, the powder pattern of the $Li_4SiO_4$ solid solutions changed continuously with increasing $x$ until it became indistinguishable from that of the $\alpha$ phase. Thus, some of the line splittings in $Li_4SiO_4$ which decrease with increasing $x$ became a single line in $\alpha$; examples are seen in Fig. 3. Crystallographic work is required to establish the structural relation between the $Li_4SiO_4$ and $\alpha$ structures and to show whether the transition is indeed continuous.

## The Phase Diagram Li₄SiO₄–LiGaSiO₄

The phase diagram (Fig. 1) shows the stability ranges of the five phases described above, four of which are solid-solution phases. These phases all have compositions on this join and the phase diagram is a binary diagram, apart from in the region of melting of $LiGaSiO_4$-rich compositions. Thus, in these compositions at some temperatures, the phase $LiGa_5O_8$ is present and its composition clearly does not lie on the title join.

Melting behavior on this join was determined from a combination of DTA, X-ray diffraction, and optical microscopy of quenched samples and the appearance of pelleted samples after heating at various temperatures. Determination of melting behavior in $LiGaSiO_4$-rich compositions was greatly helped by the occurrence of glass formation on quenching liquids containing >70% $LiGaSiO_4$. For these compositions, it was possible to heat samples isothermally, quench them into Hg, and analyze the products by optical microscopy/X-ray diffraction; the presence of glass in partially or completely melted samples was readily apparent from the microscopic examination. Hence, the eutectic temperature of 1015°C and the complex melting behavior of $LiGaSiO_4$-rich compositions was readily determined by this method. Full details of the experimental results which were used to construct the phase diagram are given in Table III (14).

## Acknowledgments

## References

1. P. W. McMILLAN, "Glass Ceramics," 2nd ed., Academic Press, New York (1979).
2. E. CHAVIRA, P. QUINTANA, AND A. R. WEST, Brit. Ceram. Trans. J. 86, 161 (1987).
3. P. QUINTANA AND A. R. WEST, Solid State Ionics 23, 179 (1987).
4. A. R. WEST, J. Appl. Electrochem. 3, 327 (1973).
5. R. D. SHANNON, B. E. TAYLOR, A. D. ENGLISH, AND T. BERZINS, Electrochim. Acta 22, 783 (1977).
6. Y.-W. HU, I. D. RAISTRICK, AND R. A. HUGGINS, J. Electrochem. Soc. 124, 1240 (1977).
7. M. MAREZIO, Acta Crystallogr. 19, 396 (1965).

8. A. R. WEST, *Z. Kristallogr.* **141**, 422 (1975).

9. A. R. WEST, AND P. G. BRUCE, *Acta Crystallogr. Sect. B* **38**, 1891 (1982).

10. J. ZEMANN, *Acta Crystallogr. Sect. B* **13**, 863 (1960).

11. G. TORRES-TREVINO AND A. R. WEST, *J. Solid State Chem.* **61**, 56 (1986).

12. A. R. WEST AND F. P. GLASSER, *J. Mater. Sci.* **5**, 557, 676 (1970).

13. D. TRANQUI, R. D. SHANNON, H.-Y. CHEN, S. IJIMA, AND W. H. BAUR, *Acta Crystallogr. Sect. B* **35**, 2479 (1979).

14. P. QUINTANA, Ph.D. thesis, Universidad Nacional Autonoma de Mexico, in preparation.